

Establishing Calibration Models and Error Envelopes of a 3D Whole Body Scanning System

YU-CHENG LIN^a, MAO-JIUN J. WANG^b AND TOLY CHEN^{c*}

^a Department of Industrial Engineering and Management
the Overseas Chinese Institute of Technology
No. 100 Chiaokwang Road, Taichung City,
Taiwan, R.O.C.

^b Department of Industrial Engineering and Engineering Management
National Tsing Hua University

^c Department of Industrial Engineering and Systems Management
Feng Chia University

http://home.kimo.com.tw/tolynet/index_e.html

Abstract: - The accuracy is important for a 3D whole body scanning system. In order to analyze the measurement error, a set of dimension-certified measurement equipment whose true dimensions were certified was introduced. The calibration models of height, breadth and depth measurement between measured values and true dimensions were established respectively and relevant error envelopes were derived. A verification experiment was conducted to determine the validity of these models. The accuracy of this scanning system can be improved by using the calibration models to obtain more accurate 3D human models.

Key-Words: - 3D whole body scanner, Calibration model, Measurement error, Error envelope, Anthropometry

1 Introduction

Traditionally, the direct measurement method, which uses contact devices, is applied to collect anthropometric data from a subject's body. However, to enhance measurement speed and to retrieve missing data are always interested [1]. The development of optical measurement method can rapidly allow measurers to collect digital 3-dimensional point clouds, produce 3D models, and take any desired data from the digital models.

As scanning technology advances and the volume of measured objects increases, measurement error analysis becomes a more serious issue, especially for the 3D whole body scanning systems. The errors are commonly caused from three sources, hardware, software and subject (human). Several studies were tried to investigate the measurement errors between traditional and optical measurement methods [2] [3], between extraction methods from scans [4], and between traditional measurement and automated measure systems [5]. All of them indicated there are significant differences. The body sway during scanning is a typical case if scanning humans. Adjusting subjects' posture and having the subjects hold their breadth could reduce this [6].

It is difficult to determine all error sources and their quantity, so suggested analysis focus is on the global measurement errors in the whole system. An

appropriate way to evaluate the global errors in a scanning system is to measure different standard objects in an adequate controlled environment [7]. If the quantity of measurement error from the whole system is determined, the dimensions can be modified using a calibration equation in the extraction program to obtain more precise information.

The accuracy of 3D system can be checked in two different ways appropriately. The first method involves measuring a precision grating with different vision angles (by moving the cameras). The second method involves measuring a standard objects whose sizes are known from different positions of the measurement field [7]. The standard object measurement method is more appropriate in evaluating the measurement error for a 3D whole body scanner. The Computerized Anthropometric Research and Design Laboratory (CARD Lab.) initiated a validation study to check the accuracy of Cyberware WB4 whole body scanner. They adopted second method involving a calibration object consisting of two boxes and a cylinder scanned at different locations in the scanning field [8]. The object dimensions calculated from the scans are compared to the actual dimensions of the calibration object. The result indicated that some acceptable measurement errors were present and no systematic

error was present in the scanning field due to the position of the calibration object.

The purpose of this study was to propose an approach for construct breadth (x-axis) and depth (y-axis) measurement calibration models for a 3D whole body scanning system. By identifying the measurement errors of the system, the breadth and depth measurement errors were independently calculated from scans using standard objects whose actual dimensions were known. Hence, the relationship between the optical measurements and true dimensions could be established. Individual breadth and depth measurement calibration models and the measurement error envelopes were also extracted respectively. These models could be employed in calibrating the scanned result and realize the distribution of errors.

2 Method

The optical measurement instrument utilized in this study was the 3D Whole Body Scanner (Vitronic, Germany). It has four scanning heads. Each head contains one laser projector, four video matrix cameras for laser reception and one color CCD. The scanning heads are moved from the top of scanner down during scanning. The sixteen video matrix cameras catch 3D point clouds on the surface of the scanned subject.

To investigate the actual measurement error for the 3D whole body scanning system, a set of dimension-certified measurement equipment was designed and manufactured. The true lengths of the pre-defined dimensions on this equipment are previously proven. It contains one stage, five standardized gauges of different lengths and a standardized holder. The stage is made of 3mm steel plate with several pillars for support. The main holder is assembled vertically on the stage and perpendicular to the standardized gauges. This equipment was utilized to determine the measurement error between the measured dimension and true dimension.

The stage is used to provide a stable foundation to locate the main holder. There are five assembly sites to locate the holder. The central assembly site is at the center of the plane on the whole stage. The "front" and "back" assembly sites are on front and back points 300 mm from the center. The "right" and "left" assembly sites are on left and right points 400 mm from the center. The assembly site coordinates are defined as (0, 0), (0, 300), (0, -300), (400, 0) and (-400, 0) respectively.

The 5 standardized gauges are employed in measuring the breadth and the depth data. The

designed lengths are 200 mm, 400 mm, 600 mm, 1000 mm, and 1200 mm respectively. They are designed to be mounted horizontally along the X-axis and Y-axis at different height on the main holder stably. The standardized gauges can be mounted on heights of 102.5 mm, 502.5 mm, 902.5 mm, 1302.5 mm, and 1702.5 mm respectively. For the purpose of evaluating the measurement error, the relevant dimensions of dimension-verifying equipment were proofed by Mechanical Industry Research Laboratory, so the true lengths of relevant dimensions were acquired. The environment of experiment was controlled to keep the temperature and humidity stable.

Due to the difficulty in determining 3D unitary measurement points in space and in orienting the scanned subjects and the characteristics of scanned data, the overall measurement error was divided into three independent axes according the axes, i.e. each axial measurement error, measurement in X (breadth), Y (depth) and Z (height) axis, was used instead of unitary one. Ignoring height, this experiment was therefore divided into two experiments, breadth (X) and depth (Y), to implement respectively. The breadth and depth measurement experiments investigated the changes in breadth and depth measurement errors occurring on different assembly sites and the mounting height of the measured gauges. The side view and top view of the assembly sites for breadth and depth measurements is illustrated in Fig. 1 and Fig. 2 respectively.

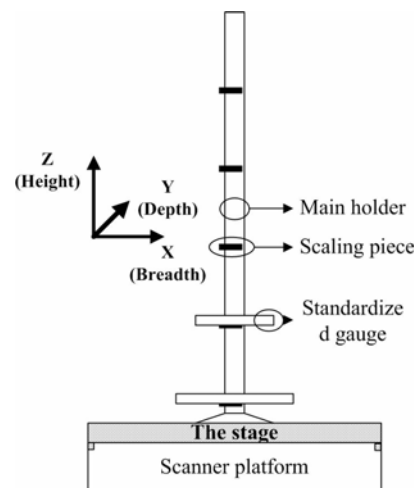


Fig. 1. The side view of the testing equipment

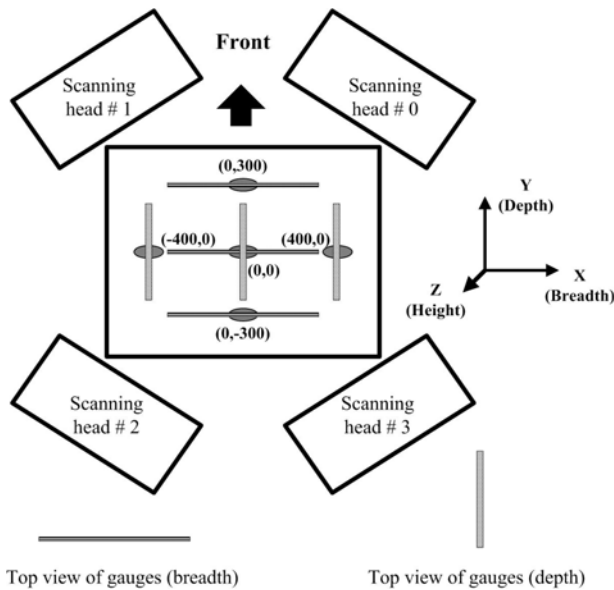


Fig. 2. The top view of the testing equipment

The independent variables of breadth measurement experiment were the assembly site (FB), standardized gauge mounting level ($M-level$) and true length of the standardized gauge ($T_X value$). The assembly sites include (0, 0), (0, 300) and (0, -300). The gauge mounting height levels are that 5 gauge height levels. The dependent variable was the measured value ($M_X data$).

The independent variables of depth measurement experiment were the assembly site (LR), standardized gauge mounting level ($M-level$) and the true length of standardized gauge ($T_Y value$). The assembly sites include (0, 0), (400, 0) and (-400, 0). The dependent variable was the measured value ($M_Y data$). A randomized experimental design with 5 repeats was adopted. Totally 375 breadth measurement samples (75 combinations) and 375 depth measurement samples (75 combinations) were taken.

3 Results

After the experiments, the scanned images were examined and some problematic scans were found. Therefore, the deformed and fragmented scans were eliminated before data analysis.

The measurement errors, the measured value minus the true dimension, under different conditions were tested to determine the statistical significance. The significant difference implies that the measurement error for the whole body scanning system is not equal to zero statistically, so the scanned result must be calibrated. After eliminating

the data from deformed and fragmented images, 70 and 55 experimental combinations for breadth measurement and depth measurement remained. For breadth measurement, 48 out of 70 experimental combinations had statistically significant differences ($\alpha= 0.05$). For depth measurement, Fifty out of 55 experimental combinations had statistically significant differences ($\alpha= 0.05$). The preliminary result indicates that the depth measurement accuracy was significantly worse than breadth measurement.

3.1 Measurement calibration models

With the breadth and depth measurement experiment results, relevant estimation models of the height measurement, breadth measurement and depth measurement were established. The idea of loss function was introduced to calculate the total loss in every possible model. The loss function is the sum of squares for the differences between the measured data and estimated dimensions (equation (1)). The less the total loss, the better the tested model. The total loss for each possible model was calculated and compared. If the total losses for two or more models were similar, the simpler model was better. Hence, the rules for selecting the optimal estimation model were to compare which model had the smaller total loss and then use the simpler model if several models have similar total losses. By reversing the models, the calibration models can be obtained.

$$Total\ Loss = \sum (Measured\ value - Estimated\ value)^2 \quad (1)$$

To consider the regular standing position in a real human scan, two different approaches for deriving estimation models are introduced and tested. First approach only considers the data measured at the central assembly site for breadth and depth measurement estimation models. The assembly site variable was therefore erased. The other approach considers all data measured on all assembly sites, so the models include the assembly site variables, FB or LR or both.

All correlation coefficients for measured data and true dimensions in tested models approximate to 1. This indicates a high linear correlation between the measured and true dimension. However, the total loss for some types of models, such as exponential type, is relatively large. These models are therefore inadequate for describing the relationship between the dependent and independent variables. If the gauge mounting level for the breadth and depth measurement is transferred into the sine function or tangent function, it is helpful for decreasing the total loss. However, its contribution is insignificant. All

models listed below are the best one in our picking the related optimal model trial process.

3.2 breadth measurement calibration model

The best estimation model established with the data from the central assembly site only (ignoring the assembly site) was compared with another best model considering using all of the data (consider the assembly site). Both models have high variance explained. The amounts of total loss are 282 and 509 respectively. According to the variance explained, the contribution of mounting level (*M – level*) is insignificant so it is excluded from models. However, the assembly site is an important since the location of the scanned objects is various actually. Thus, the estimation model considering the assembly site should be more reasonable. By reversing this estimation model, the calibration model for the breadth measurement was obtained (model (2)).

Calibration model:

$$T_x \text{ value} = 54623.02 - 330.82 \times (27265.43 + 0.001 \times FB - 0.00001 \times FB^2 - M_x \text{ data})^{0.5} \quad (2)$$

3.3 depth measurement calibration model

The result is similar to that of breadth measurement. The contribution of mounting level (*M – level*) is still insignificant. Both models established with different data sets have high variance explained and the one ignoring assembly site variable still has less total loss. However, the total loss for this model becomes larger if all of the experimental data was inputted. Hence, the estimation model should include the assembly site variable. By reversing the model including the assembly site variable, the calibration model for the breadth measurement was obtained (Model (3)).

Calibration model:

$$T_y \text{ value} = 3016.52 - 74.195 \times (1641.6011 - 0.0053 \times LR + 0.00003 \times LR^2 - M_y \text{ data})^{0.5} \quad (3)$$

Because the global measurement error is divided into independent axial measurement errors to derive the models, the true Y and Z coordinate of a 3D point can be calculated with relevant calibration models. An experiment without the stage was conducted to validate the models using a manikin. Eight linear dimensions were measured from the manikin both with the whole body scanner and a precise 3D coordinate measuring probe, whose precision is less than 0.01 mm. The data measured by the probe was treated as true value. The result showed 7 out of 8

dimensions had statistically significant difference in means. The data was calibrated with the models. The result indicated only 1 out of 8 dimensions still had statistically significant difference. The validity of calibration models was verified.

3.4 Establishing the measurement error envelopes

The ranges and envelopes of the measurement errors were established based on the breadth and depth measurement calibration models. The measurement error ranges along each axis for breadth (X-axis) and depth (Y-axis) were obtained from the corresponding models. The breadth and depth measurement errors can be considered plane measurement errors (X-Y plane) and are independent of the height. The corresponding error contours can be derived according to the measurement error ranges and estimation models. Fig. 3 and Fig. 4 illustrate the top views of the breadth and depth measurement error contours respectively. Combining different breadth and depth measurement error ranges forms a closed space where the measurement errors are divided into different intervals, that is, the measurement error envelopes. Figure 5 and 6 reveal various envelopes formed by different breadth and depth error ranges. The two figures illustrate the boundaries of the error envelopes. Because of the variety in the breadth and depth measurement errors, one error envelope may involve another one or be involved by another one. For example, Fig. 6 illustrates the single envelope whose plane error boundary is -2 mm. Inside the rectangular cube, all absolute measurement error values are less than 2 mm. Outside the cube, absolute measurement error values are greater than 2 mm.

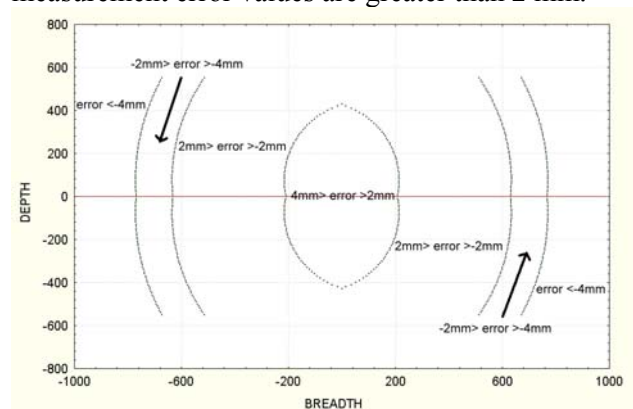


Fig. 3. Top view of the breadth measurement error contours

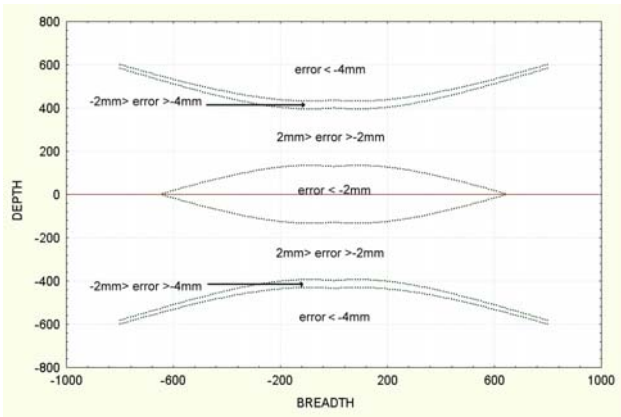


Fig. 4. Top view of the depth measurement error contours

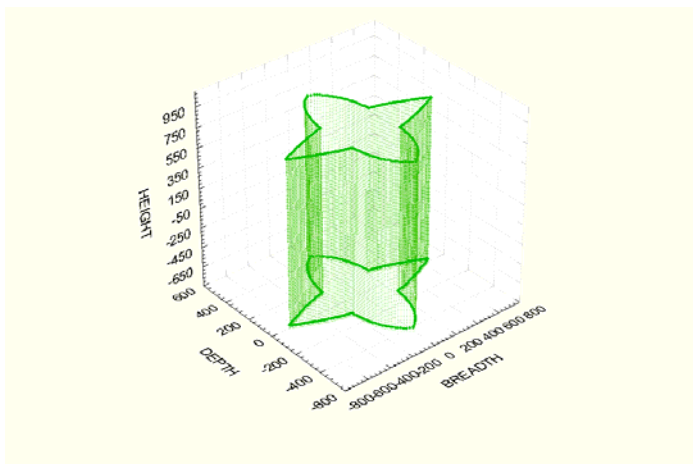


Fig. 5. Illustration of the single envelope whose height error boundary is -4 mm and absolute plane error boundary value is 2 mm.

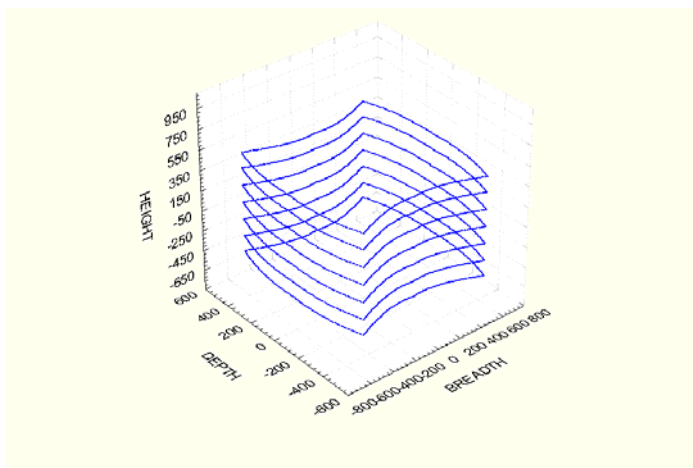


Fig. 6. Illustration of the single envelope whose height error boundary is -2 mm and plane error boundary is -2 mm.

By combining two single error envelopes (Fig. 5 and Fig. 6), the measurement status for the 3D whole body scanner is more clearly represented. Fig. 7 is a

composite illustration of two envelopes whose absolute plane error boundary values are 2 mm. Inside the star cube, at least one of the absolute breadth and depth measurement error values is greater than 2 mm. Outside the rectangular cube, all of the absolute measurement error values are greater than 2 mm. The absolute plane error value between two cubes is less than 2 mm.

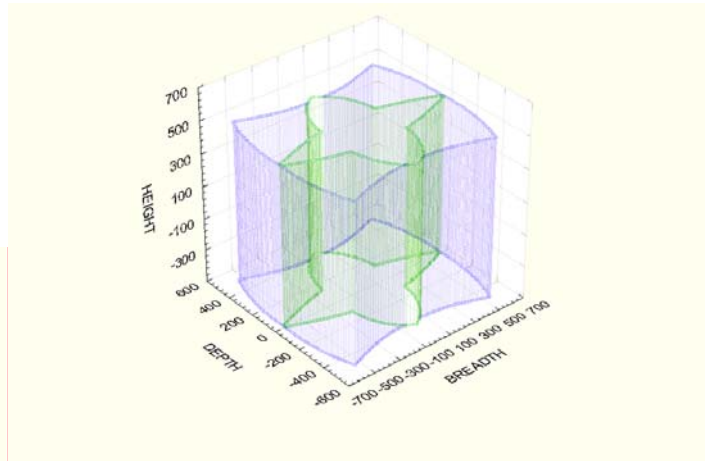


Fig. 7. Illustration of two envelopes whose height error boundaries are both -2 mm and absolute plane error boundary values are 2 mm.

4 Discussion

The change in measurement error and their distribution patterns are regular. This can be observed clearly from the estimation models and Fig. 3 and Fig. 4. The extremely large variance explained in each estimation model indicates that the estimation is good. The variation ranges in most measurement errors obtained in this experiment were within millimeters. It is small compared to the size of a human. This may be another reason for the high variance explained.

The breadth measurement error convex contour shape reflects the optimal camera measurement field (Fig. 3). The measurement error varies from 2 mm to 4 mm in the central oval part of the contours because this region is distant from all of the scanning heads. The measurement error becomes smaller if the distance between the object and camera is appropriate. The measurement error becomes large as the scanned object is much farther from the center. Although the breadth error along X-axis is also greater than 4 mm outside 768 mm from origin, it already surpasses 1100 mm, the designed breadth scanning field in breadth ($768 \times 2 = 1536 > 1100$).

Similarly, the depth measurement error concave contour shape reflects the distribution of optimal measurement field (Fig. 4). The absolute

measurement error value is larger than 2 mm (even more than 4 mm) in the central closed elliptical contour because this region is distant from all of the scanning heads. Leaving the central area, the distance between the object and the camera becomes appropriate and the measurement error is within a range from -2 mm to 2 mm. The measurement error becomes large as the distance from the center is too long. The long distance from center means the distance between the surface of the object and the cameras is either too short or too far. Although the absolute depth error value along Y-axis is also greater than 4 mm outside a 435 mm distance from the origin and is less than 1100 mm, the designed depth scanning field, it satisfies the application in human body scan.

Regardless of the calibration models, facing to the corner of the cube (Fig. 6) seems a better scan facing direction based on the consideration of minimizing the measurement error. The intersection of the subject body and the star-shape area becomes much smaller but the intersection of the subject body and the area between the rectangular cube and star cube is larger. Thus, the amount of the 3D points that fall in the area between the two cubes is increased. That is, the measurement error is reduced without the calibration process. In practice, a more appropriate way to take more accurate scans is to ask the subject to face to a specific camera or the central line of a specific scanning head. The measurement error can be reduced and the system accuracy can be enhanced with the change in standing facing direction.

5 Conclusion

For the error analysis of 3D whole body scanning system, an experiment was proposed with a set of dimension-certified measurement equipment that true dimension were obtained. Most of measurement error, the value of measured data extracted from scans minus related true dimension, was not equal to zero significantly. So the estimation models of breadth and depth measurements were established. Based on the estimation models, relevant calibration models of breadth and depth measurement were obtained and they can be utilized to improve the measurement error. A simple validation experiment indicated the validity of calibration models was adequate to reduce the difference between true value and estimated value.

Based on the estimation models, the contours of breadth and depth measurements were illustrated. The 3D error envelopes were obtained by combining different error boundaries. A star-shape cubic exists in central area of scanning field and the breadth and

depth measurement error is greater inside the cube than outside. This area should be covered by scanned object to take more accurate measurements. An optimal measurement range from -631 to 631 mm in breadth and -399 to 399 mm in depth was suggested. Furthermore, the new facing direction, the front, is strongly suggested. The subjects should stand near the center of platform and face to a specific camera or the central line of a specific scanning head during scanning to reduce measurement error. Hence, the scanned result along X and Y by 3D whole body scanning system can be more accurate with calibration models and the new facing direction.

References:

- [1] J. A. Roebuck, Anthropometric methods: Designing to Fit the Human Body, CA: Human Factors and Ergonomics Society, Santa Monica, 1995, 25-46, 53-61.
- [2] P. Meunier, S. Yin, Performance a 2D image-based anthropometric measurement and clothing sizing system, Applied Ergonomics, Vol. 31, 2000, 445-451.
- [3] Y. H. Wu, J. Y. Lin, Y. C. Lin, Evaluating the Use of the 3-D Whole Body Scanner to Collect Anthropometric Data for the Development of Automated Tailoring System, Journal of Industrial Engineering Design Vol. 4, 2002, 4-6.
- [4] L. Dekker, Custom-made clothing, Proceedings of 3D anthropometric technology and application, China Textile Institute, 2000, 6-8.
- [5] S. Paquette, D. Brantley, B. D. Corner, P. Li, T. Oliver, Automated Extraction of Anthropometric Data from 3D Images, Proceedings of the IEA 2000/ HFES 2000 Congress, 2000, 727-730.
- [6] M. A. Brunsmann, H. M., Daanen, K. M. Robinette, Optimal postures and positioning for human body scanning, Proceedings of International Conference on 3D Digital Imaging and Modeling, 1997, 226-273.
- [7] J. J. Aguilar, F. Torres, M. A. Lope, Stereo vision for 3D measurement: accuracy analysis, calibration and industrial applications, Measurement, Vol. 18, 1996, 193-200.
- [8] H. A. Daanen, S. E. Taylor, M. A. Brunsmann, J. H. Nuure, Absolute accuracy of the Cyberware WB4 whole-body scanner, Proceedings of the SPIE, 3023, 1997, 6-12.